Overview and early results of the Superconducting Submillimeter-Wave Limb-Emission Sounder (SMILES)

Ken-ichi Kikuchi,[1] Toshiyuki Nishibori,[1] Satoshi Ochiai,[2] Hiroyuki Ozeki,[3] Yoshihisa Irimajiri,[2] Yasuko Kasai,[2] Makoto Koike,[4] Takeshi Manabe,[5] Kazuo Mizukoshi,[1] Yasuhiro Murayama,[2] Tomoo Nagahama,[6] Takuki Sano,[7] Ryota Sato,[1] Masumichi Seta,[8] Chikako Takahashi,[7,9] Masahiro Takayanagi,[1] Harunobu Masuko,[2] Junji Inatani,[10] Makoto Suzuki,[7] and Masato Shiotani[11]

[1]   The Superconducting Submillimeter-Wave Limb-Emission Sounder (SMILES) was successfully launched and attached to the Japanese Experiment Module (JEM) on the International Space Station (ISS) on 25 September 2009. It has been making atmospheric observations since 12 October 2009 with the aid of a 4 K mechanical cooler and superconducting mixers for submillimeter limb-emission sounding in the frequency bands of 624.32–626.32 GHz and 649.12–650.32 GHz . On the basis of the observed spectra, the data processing has been retrieving vertical profiles for the atmospheric minor constituents in the middle atmosphere, such as O_3 with isotopes, HCl, ClO, HO_2, BrO, and HNO_3. Results from SMILES have demonstrated its high potential to observe atmospheric minor constituents in the middle atmosphere. Unfortunately, SMILES observations have been suspended since 21 April 2010 owing to the failure of a critical component.

Citation: Kikuchi, K., et al. (2010), Overview and early results of the Superconducting Submillimeter-Wave Limb-Emission Sounder (SMILES), *J. Geophys. Res.*, *115*, D23306, doi:10.1029/2010JD014379.

1.   Introduction

[2]   The Superconducting Submillimeter-Wave Limb-Emission Sounder (SMILES) was developed to be aboard the Japanese Experiment Module (JEM) on the International Space Station (ISS) through the cooperation of the Japan Aerospace Exploration Agency (JAXA) and the National Institute of Information and Communications Technology (NICT). SMILES was successfully launched by an H-IIB rocket with the H-II Transfer Vehicle (HTV) on 11 September 2009, was attached to the JEM on 25 September, and began atmospheric observations on 12 October (all dates in JST hereafter, unless otherwise specified).

[3]   The mission objectives are as follows: (1) to demonstrate a 4 K mechanical cooler and superconducting mixers in the environment of outer space for submillimeter limb-emission sounding in the frequency bands of 624.32–626.32 GHz and 649.12–650.32 GHz and (2) to measure atmospheric minor constituents in the middle atmosphere globally (O_3, HCl, ClO, HO_2, HOCl, BrO, O_3 isotopes, HNO_3, CH_3CN, etc.) to gain a better understanding of factors and processes controlling the stratospheric ozone amounts and those related to climate change. (For more details, see the SMILES Mission Plan, version 2.1, at http://smiles.tksc.jaxa.jp/document/SMILES_MP_ver2.11.pdf.)

[4]   High-sensitivity measurement of minor species is expected to be performed by a receiver using superconductor-insulator-superconductor (SIS) mixers, cooled to 4.5 K by a compact mechanical cryocooler. The cryocooler, a Joule–Thomson circuit and a two-stage Stirling refrigerator developed and equipped for atmospheric observation from space for the first time, shares a heritage with the X-ray astronomical satellite ASTRO-H [*Takahashi et al.*, 2008] and the Space Infrared Telescope for Cosmology and Astrophysics (SPICA) [*Onaka and Nakagawa*, 2005].

[5]   The main scientific target of the SMILES mission is to study the recovery and stability of the stratospheric ozone layer. Coupled chemistry-climate model (CCM) calculations have suggested that global (60°S–60°N) ozone levels

[1]ISS Science Project Office, Tsukuba Space Center, Japan Aerospace Exploration Agency, Tsukuba, Japan.
[2]National Institute of Information and Communications Technology, Koganei, Japan.
[3]Department of Environmental Science, Faculty of Science, Toho University, Funabashi, Japan.
[4]Department of Earth and Planetary Physics, Graduate School of Science, University of Tokyo, Tokyo, Japan.
[5]Department of Aerospace Engineering, Graduate School of Engineering, Osaka Prefecture University, Sakai, Japan.
[6]Solar-Terrestrial Environment Laboratory, Nagoya University, Nagoya, Japan.
[7]ISS Science Project Office, Institute of Space and Astronautical Science, Japan Aerospace Exploration Agency, Sagamihara, Japan.
[8]Institute of Physics, University of Tsukuba, Tsukuba, Japan.
[9]Also at Fujitsu FIP Cooperation, Tokyo, Japan.
[10]National Astronomical Observatory of Japan, Mitaka, Japan.
[11]Research Institute for Sustainable Humanosphere, Kyoto University, Uji, Japan.

will recover to pre-1980 levels around the middle of the twenty-first century [*World Meteorological Organization (WMO)*, 2007]. However, there are still considerable uncertainties in factors affecting ozone levels, especially the bromine budget and inorganic chlorine chemistry. Stratospheric cooling due to increases in greenhouse gases and possible changes in transport processes induced by radiative forcing could also affect the trend and stability of the ozone layer. A recent study showed that there were substantial quantitative differences in the recovery time of Antarctic springtime column ozone among projections from eleven CCMs, although they employed the same emission scenarios [*Eyring et al.*, 2007]. Because the SMILES mission is identified as one focusing on the detailed halogen chemistry related to ozone destruction, we aim at providing useful constraints for these issues, as described in the rest of this section.

[6] Recent BrO measurements suggest that in addition to long-lived source gases (halons and methyl bromide), very short-lived (<6 months) source gases likely contribute to stratospheric total inorganic bromine (Br_y) by about 5 parts per trillion by volume (pptv) [*WMO*, 2007]. These additional Br_y sources can be important for O_3 chemistry because they increase the relative importance of BrO-catalytic O_3 loss cycles in the lower stratosphere, especially under high aerosol loading conditions, leading to a better agreement with the observed O_3 trend in the northern midlatitudes [*Salawitch et al.*, 2005]. So far, only two satellite sensors have provided global distribution of stratospheric BrO [*Sinnhuber et al.*, 2005; *Livesey et al.*, 2006a], and consequently, BrO measurements by SMILES are expected to provide further constraints on the Br_y level.

[7] Partitioning within Cl_y is important for the O_3 trend at midlatitudes, as well as in the polar region, because the ClO_x (Cl + ClO) level is essential for the O_3 loss rate. For the O_3 trend in the upper stratosphere, it has been suggested that inclusion of an HCl yield of about 6% from the reaction of ClO + OH results in a better agreement with the observed O_3 trend at northern midlatitudes as well as observed ratios within Cl_y species [*WMO*, 1999]. Reevaluation of the rate constant of the reaction ClO + $HO_2 \rightarrow$ HOCl + O_2 is also important because this reaction is the rate-limiting step of the O_3 loss cycle including HOCl and because it could be a factor of about two greater than the Jet Propulsion Laboratory (JPL) 2006 recommendation [*Kovalenko et al.*, 2007]. The ClO + HO_2 cycle can be the most efficient O_3 loss process within the cycles involving ClO in the lower stratosphere. SMILES measurements of the absolute concentration of HCl are also essential to monitor the Cl_y level in the stratosphere. Because of the high sensitivity described in section 3, SMILES will provide accurate global datasets of ClO, HCl, HOCl, and HO_2 concentrations, which will provide important insights into inorganic chlorine chemistry and the O_3 trend.

[8] In addition to these halogen-related themes, we will investigate other scientific objectives in the middle atmosphere, including the HO_x budget [e.g., *Canty et al.*, 2006] and ozone isotope distributions [e.g., *Krankowsky et al.*, 2007]. We will also try to study climate change related issues by SMILES observations of ice clouds and water vapor in the upper troposphere and the lower stratosphere that play significant roles in the radiation budget of the Earth

system. Ice clouds can also serve as a site of heterogeneous reactions. In addition, dynamical and transport processes affecting the distribution of minor species will be important topics to be studied.

[9] Since the ISS has a circular orbit with an inclination angle of 51.6°, no observations in the polar latitudes are available. To measure northern high-latitude regions, the antenna beam is tilted 45° left from the direction of orbital motion, enabling SMILES to observe latitudes from 38°S to 65°N. Another important aspect of SMILES observations is that SMILES can measure the atmosphere at different local times because of the non-sun-synchronous ISS orbit. Measurements of diurnal variation of the aforementioned minor species are expected to provide further insights into the atmospheric chemistry.

[10] Unfortunately, SMILES observations have been suspended since 21 April 2010 owing to the failure of a critical component in the submillimeter local oscillator. Possible repair strategies are being considered, as it is on the space station. During the operational mode, SMILES had been performing global observations at about 100 locations per ISS orbit, except for some restrictions due to ISS operation. After data processing, global and vertical distributions of about 10 atmospheric minor constituents related to the ozone chemistry are derived, which will contribute to various issues of atmospheric science described above.

[11] In this paper, an overview of the SMILES instrument and observations will be documented with some early observational results. In section 2, we provide information on the ISS platform and the Japanese Experiment Module. Descriptions of the SMILES instrument will be found in section 3. Section 4 will summarize the dataflow and processing, including the algorithm theoretical basis, ground data processing system, and expected performance. In section 5, we will present some preliminary results that demonstrate SMILES's abilities to observe the atmospheric minor constituents in the middle atmosphere. Section 6 provides a brief summary of these preliminary results.

2. Platform

[12] SMILES was carried on the H-II Transfer Vehicle (HTV) and launched by the Japanese H-IIB launch vehicle. The HTV is a Japanese unmanned cargo spacecraft, which can carry up to six tons of cargo under both pressurized and unpressurized conditions. The launch of SMILES, which was the first flight for both the H-IIB launcher and HTV spacecraft, was conducted on 11 September 2009 from Tanegashima Space Center in Japan.

[13] The HTV was docked to the ISS on 18 September after initial engineering tests of the HTV as a spacecraft. The ISS is a large manned laboratory orbiting about 400 km above the Earth's surface. It is in a nearly circular orbit with an inclination of 51.6° to the equator and a period of about 90 min. The Japanese Experiment Module (JEM), Kibo, one of the modules connected to the ISS node, consists of two facilities: the Pressurized Module (PM) and the Exposed Facility (EF). Currently, there are four science and engineering missions under operation on the JEM/EF: Monitor of All-sky X-ray Image (MAXI) [*Mihara et al.*, 2000]; Space Environment Data Acquisition Equipment-Attached Payload (SEDA-AP) [*Koga et al.*, 2001]; and HICO and
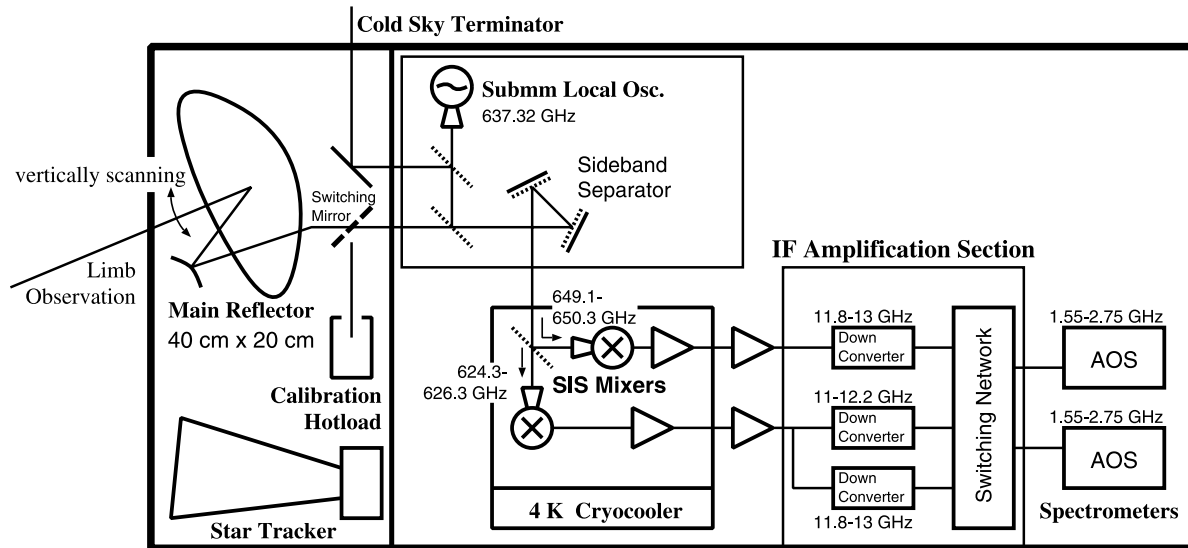
Figure 1. Block diagram of SMILES instrument. See text (subsection 3.1) for details.

RAIDS Experiment Payload (HREP) from NASA and SMILES. JEM/EF can accommodate up to two system modules and nine experimental modules, each of which is 500 kg or larger. The JEM/EF has a data rate of up to 100 Mbps telemetry and a 10 kW power supply.

[14] SMILES was attached to the third port of the Exposed Facility Unit (EFU) of the JEM on 25 September. Soon after the attachment, the 4 K cooler system was turned on; it successfully reached below 4.5 K on 28 September. The first operator-initiated observation was attempted on 10 October, but only a few profiles were taken. The first continuous observation of the Earth's atmosphere was carried out on 12 October, and SMILES performed atmospheric observations since then, except for restrictions due to ISS operation conditions, until SMILES observations were suspended on 21 April 2010.

3. Instrument Description and Operation of SMILES

3.1. SMILES Instrument

[15] The SMILES concept dates back to the late 1980s; it was proposed to the National Space Development Agency of Japan (NASDA, now JAXA) in the early 1990s by *Masuko et al.* [1997]. In 1997, SMILES was accepted as a candidate to be an early science mission of the ISS/JEM. There had been contributions from the European science community based upon the heritage of the Millimeter-wave Atmospheric Sounder (MAS) experiment on board the space shuttle [*Hartmann et al.*, 1996; *Buehler et al.*, 1999]. This section briefly describes the SMILES instrument. (Details can be found in the SMILES Mission Plan, version 2.1, at http://smiles.tksc.jaxa.jp/document/SMILES_MP_ver2.11.pdf.)

[16] Figure 1 shows a block diagram of the SMILES instrument [*Inatani et al.*, 2000; *Masuko et al.*, 2000; *Seta et al.*, 2000]. An offset Cassegrain antenna with an elliptical primary reflector, whose major and minor axes are 40 cm (elevation) and 20 cm (azimuth) in diameter, gives an instantaneous field of view (IFOV) of 0.09° (~3 km) in

elevation [*Manabe et al.*, 2008; *Manabe et al.*, 2010]. Details of the antenna scan are given in section 3.2.

[17] Two superconductor-insulator-superconductor (SIS) mixers are cooled to 4 K using a two-stage Stirling cycle cooler and a Joule–Thomson (JT) cooler [*Narasaki et al.*, 2004]. The SIS mixers convert the submillimeter signal to the first intermediate frequency (IF) in the 11.0–13.0 GHz region by mixing with the output of a local oscillator operating at 637.32 GHz. A quasi-optical sideband separator [*Inatani et al.*, 1999; *Manabe et al.*, 2003] inserted between the antenna and the SIS mixer gives an image band rejection of better than 20 dB. The IF signal is further down-converted to the second IF in the 1.55–2.75 GHz region. The frequency spectra of the signal are obtained by two sets of acousto-optical spectrometers (AOSes), each of which has 1728 spectrometer channels [*Ozeki et al.*, 2000].

[18] Within the submillimeter-wave region from 625 GHz to 650 GHz, SMILES measures three specified detection bands: 624.32–625.52 GHz (Band A), 625.12–626.32 GHz (Band B), and 649.12–650.32 GHz (Band C). The SMILES instrument contains only two AOS spectrometers. Accordingly, observations of Bands A, B, and C are made on a time-sharing basis. Table 1 lists the specifications of the SMILES instrument. Although the operational lifetime of SMILES is specified to be 1 year, several subsystems of the SMILES engineering model, such as the cryocooler, have been tested and found to operate much longer than 1 year under laboratory conditions.

3.2. Operation of SMILES

[19] SMILES observes the Earth's limb from the ISS at a typical altitude between 350 and 400 km, and the distance from SMILES to the tangent point (30 km in altitude) ranges between 2050 and 2200 km. Since the ISS orbit is a circular one with an inclination of 51.6° to the equator, the highest latitude reached by the ISS orbit is 52° north and south. To extend the latitudinal coverage to the northern polar region, the SMILES antenna is mounted so that its field of view is 45° to the left of the orbital plane. SMILES limb-sounding

Table 1. Specifications of the SMILES Instrument

	Specified Value
Frequency coverage	Band A: 624.32–625.52 GHz
	Band B: 625.12–626.32 GHz
	Band C: 649.12–650.32 GHz
Frequency sampling	0.8 MHz
Frequency resolution	~1.1–1.2 MHz (full width at half maximum)
System noise temperature	~350 K
Integration time	0.5 s for each observation tangent point
Noise level in brightness temperature	<0.7 K (for 0.5 s integration time)
Calibration accuracy	<1.0 K (for 0.5 s integration time)
Observation cycle	53 s
Observation altitude range	10–60 km (nominal)
Vertical sampling	~2 km (nominal)
Instrumental height resolution (IFOV)	3.5–4.1 km (nominal)
Observation latitudes	38°S–65°N (nominal)
Observation azimuth angle	−10–95° (0 = north)
Power consumption	~320 W (at beginning of life)
Payload weight	476 kg
Payload size	0.8 m (W) × 1 m (H) × 1.85 m (L)

observation with this field-of-view deflection provides a latitudinal coverage 65°N to 38°S on each orbit.

[20] The antenna is scanned in elevation at a period of 53 s, of which the first 29.5 s is allocated to limb atmospheric measurements to cover a tangent-height range of 10–60 km (Figure 2). The AOS integrates the spectra over 0.5 s, while the antenna is scanned stepwise at a rate of 0.009375°/s per 1/12 s, so the actual IFOV is the summation of six different antenna IFOVs over 0.5 s. After the atmospheric limb measurement for 29.5 s, the antenna is pointed toward the sky higher than 160 km to make reference cold sky observations for a nominal duration of 4 s, and then the receiver input is terminated to an ambient temperature load for 4 s, both for calibration. The radiometric sensitivity and calibration accuracy for signals from a thin atmosphere (T_b < 20 K) were estimated to be better than 0.7 K and 1.0 K, respectively. The mechanical pointing of the antenna is determined from the data on the ISS GPS position with an accuracy of 100 m (1 sigma) for each dimension, ISS attitude and/or SMILES attitude (0.006° or 210 m), and the readout of the antenna scan angle resolver (0.0015° or 60 m). The expected tangent altitude knowledge precision is ~340 m (1 sigma) (see the SMILES Mission Plan, version 2.1, at http://smiles.tksc.jaxa.jp/document/SMILES_MP_ver2.11.pdf).

[21] Along one 91 min orbit, SMILES takes measurements at about 100 points, and the total number per day is about 1600. Unfortunately, the rotating ISS solar paddles intersect the SMILES field of view twice each orbit. Occurrence of the solar paddle interference is estimated to be a few percent, depending on the latitude range, but it is not negligible. It will be described in section 4 by showing observation points in Figure 6. Moreover, around the first half of December 2009, for about two weeks, the solar paddles stayed at a fixed position and the field of view of the SMILES antenna was completely blocked by the paddles, resulting in consecutive missed observations. Such conditions of SMILES operation are noted in the observation status calendar shown in Figure 3.

3.3. Performance of SMILES

[22] Figure 4 shows examples of brightness temperature spectra in Bands A, B, and C for several tangent altitudes obtained in the first-light observation after launch. Band A (Figure 4a) includes strong ozone and $H^{37}Cl$ lines with other minor peaks of HOCl, HNO_3, ^{81}BrO, and ozone isotopes. The noise level of the brightness temperature is found to be ~0.4 K, which is lower than its specification (0.7 K). The spectral frequencies agree with the line parameter database within 100 kHz precision, after a Doppler correction taking the ISS motion and the Earth's rotation into account. At first glance, the preliminary data indicate that the short- and long-term calibration stabilities seem to be good. Further verification is needed to assess the calibration stability. Band B (Figure 4b) is somewhat similar to Band A with strong ozone and $H^{35}Cl$ lines. Additionally, there are lines for HO_2 and some ozone isotopes. Band C (Figure 4c) is in a window region and has no strong emission line within the observation frequency band. The spectral lines of ClO, HO_2, ^{81}BrO, HNO_3, and some ozone isotopes are observed in Band C. Though the ^{81}BrO line in Band C is overlapped by the ^{17}OOO line, it is found that the ^{81}BrO retrieval in Band C is more promising than that from Band A, in which it is overlapped by the HNO_3 line, since ^{17}OOO information can be derived within Band C. Concentrations of BrO and HCl are calculated from the natural abundance of the isotopic compositions by referring to *De Laeter et al.* [2003].

[23] Observed spectra at 15 km show that the emission lines of O_3 and HCl can be detected, but they are quite broad, and so SMILES lacks sensitivity for the troposphere. There is no observable H_2O line in the SMILES observation bands, but the detection of H_2O continuum and/or cirrus clouds around the tropopause are possible owing to the continuum spectra.
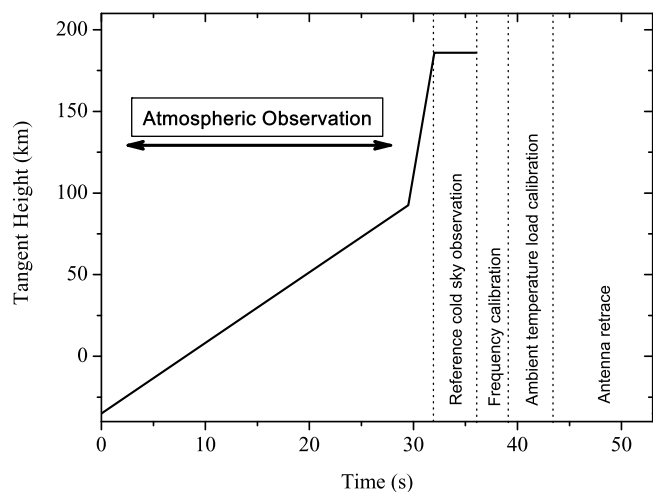

Figure 2. SMILES operational antenna scan profile. The tangent height of the FOV bore sight is shown; it is calculated with the condition of ISS nominal altitude (400 km) and attitude. The antenna scan period is 53 s. The first 29.5 s is allocated to limb atmospheric measurements; the rest of the scan period is used for reference cold sky observation, frequency calibration, ambient temperature calibration, and antenna retrace to the initial position.
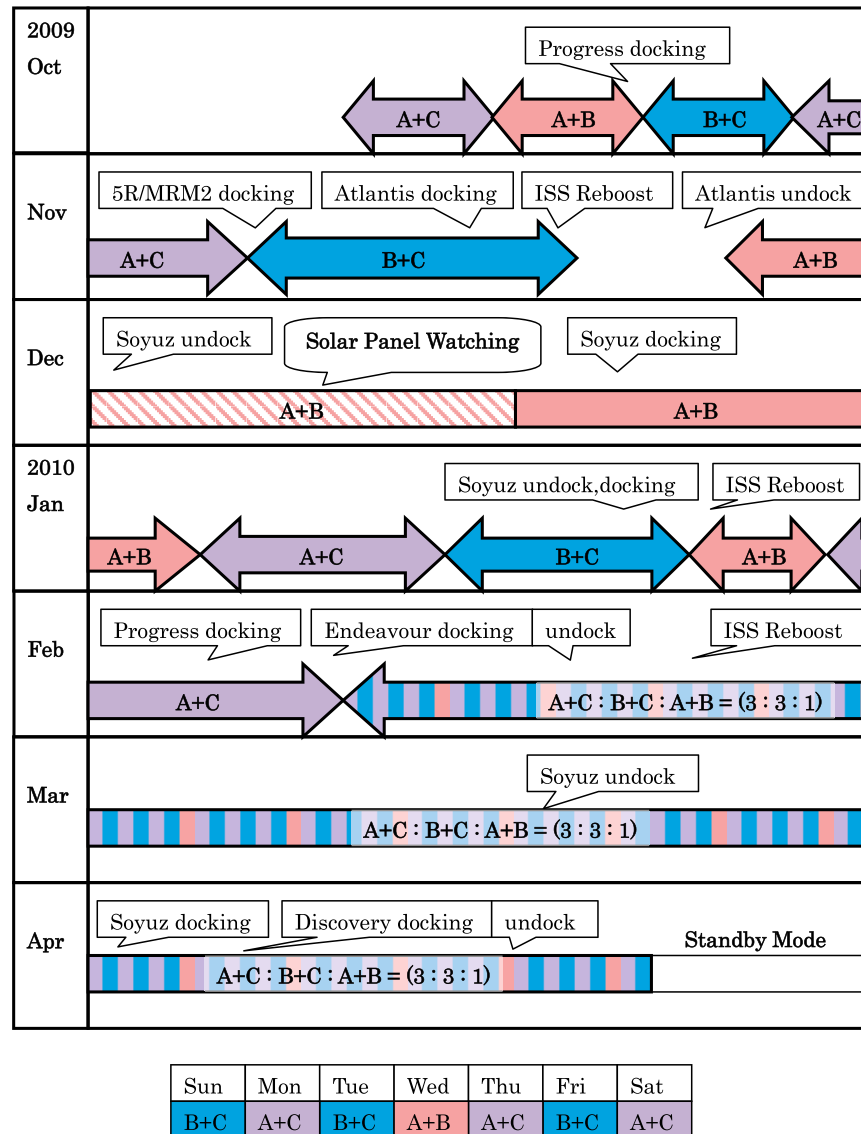
Figure 3. SMILES observation status calendar. As indicated in the weekly sequence, cyclic observations were performed with a combination of the three bands in the last 2 months or so.

[24] The system noise temperature (T_{sys}) during the initial measurements in orbit is approximately 350 K, which is much lower than its design target of 500 K. The observation noise is given by both T_{sys} and the emission from the atmosphere (T_{atm}),

$$\Delta T = \frac{T_{sys} + T_{atm}}{\sqrt{\Delta\nu \cdot \tau}} \qquad (1)$$

where $\Delta\nu$ is the spectral band width, and τ is the integration time. The SMILES receiver, equipped with the 4.5 K cooled SIS mixer, achieves a significant improvement in the sensitivity of atmospheric limb observations in the millimeter and submillimeter regions over the conventional Aura Microwave Limb Sounder (MLS) [*Waters et al.*, 2006; *Jarnot et al.*, 2006] and Odin submillimeter microwave radiometer (SMR) [*Murtagh et al.*, 2002; *Frisk et al.*, 2003] receivers. In fact, the observation noise of SMILES is ~0.45 K when

assuming T_{sys} = 400 K, T_{atm} = 50 K, τ = 0.5 s, and $\Delta\nu$ = 2 MHz. Those of Odin-SMR and Aura MLS are ~2.4 K (T_{sys} = 3300 K for the 541–581 GHz band, τ = 1.85 s, and $\Delta\nu$ = 1 MHz) and ~4.2 K (T_{sys} = 4200 K for the 640 GHz band, τ = 0.161 s, and $\Delta\nu$ = 6 MHz), respectively.

4. Dataflow and Processing

4.1. Retrieval Algorithm

[25] The SMILES retrieval algorithms and their sensitivities have been studied in a series of investigations [*Buehler*, 1999; *Buehler et al.*, 1999; *Takahashi et al.*, 2000; *Kasai et al.*, 2000; *Verdes*, 2002; *Buehler et al.*, 2005; *Melsheimer et al.*, 2005; *Ochiai et al.*, 2005; *Kasai et al.*, 2006; see also SMILES Mission Plan, version 2.1, at http://smiles.tksc.jaxa.jp/document/SMILES_MP_ver2.11.pdf].

[26] The retrieval algorithm in the operational processing chain [*Takahashi et al.*, 2010] employs the optimal estimation
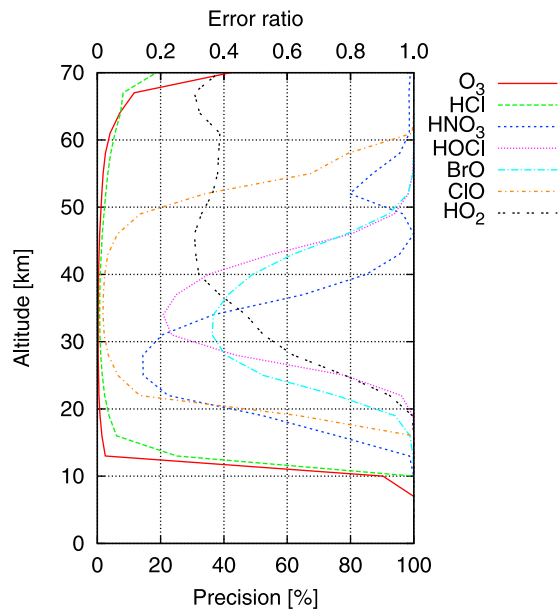
Figure 4. Observed spectra at several altitudes for (a) Band A, (b) Band B, and (c) Band C. Band A and C measurements were done at 03:22:14 UT on 12 October 2009 at 23.30°N and 173.83°E. Band B measurements were made at 00:53:32 UT on 17 October at 21.52°S and 138.83°E; latitude/longitude and time information is defined at 30 km along the scan.

Figure 5. Retrieval precision of the target species O_3, HCl, HNO_3, HOCl, BrO, ClO, and HO_2, retrieved from single-scan data in the daytime. The retrieval precision is expressed by the error ratio (σ/σ_a).

method (OEM) applied to atmospheric remote sensing [*Rodgers*, 1976, 1990, 2000]. The most probable solution is derived from statistical combination of a priori knowledge of the atmospheric state and information of the measurement. We use the Levenberg–Marquardt method [*Levenberg*, 1944; *Marquardt*, 1963] to obtain the solution. The ith iteration can be expressed as

$$\mathbf{x}_{i+1} = \mathbf{x}_i + \left(\mathbf{S}_a^{-1} + \mathbf{K}_i^{\mathbf{T}}\mathbf{S}_y^{-1}\mathbf{K}_i + \gamma\mathbf{S}_a^{-1}\right)^{-1}$$
$$\cdot \left\{\mathbf{K}_i^{\mathbf{T}}\mathbf{S}_y^{-1}[\mathbf{y} - \mathbf{F}(\mathbf{x}_i)] + \mathbf{S}_a^{-1}[\mathbf{x}_a - \mathbf{x}_i]\right\} \qquad (2)$$

where $\mathbf{x}$ is the state vector, $\mathbf{y}$ is the measurement vector, and $\mathbf{F}$ is the forward model to describe the physics and measurement process value by using the atmospheric state and the instrument characteristics. A priori knowledge about the mean $\mathbf{x}_a$ of $\mathbf{x}$, and its covariance $\mathbf{S}_a$ is used to obtain solutions in the standard OEM. $\mathbf{S}_y$ is the diagonal covariance matrix of the measurement vector, $\mathbf{K}_i$ is the matrix of weighting functions calculated for the atmospheric state $\mathbf{x}_i$, and γ is the adjusting parameter of Marquardt's iteration.

[27] The SMILES forward model carefully takes account of the atmospheric radiation and the instrument characteristics as precisely as possible [*Takahashi et al.*, 2010; *Imai et al.*, 2010; see also the SMILES Mission Plan, version 2.1, at http://smiles.tksc.jaxa.jp/document/SMILES_MP_ver2.11. pdf]. The forward model of the current retrieval was designed to have a target precision of 10^{-3} K precision.

4.2. Expected Sensitivity

[28] The precision of the retrieval is given by

$$\mathbf{S} = \left(\mathbf{K}^{\mathbf{T}}\mathbf{S}_y^{-1}\mathbf{K} + \mathbf{S}_a^{-1}\right)^{-1} = \mathbf{S}_m + \mathbf{S}_n \qquad (3)$$

where

$$\mathbf{S}_m = \mathbf{G}\mathbf{S}_y\mathbf{G}^{\mathbf{T}}, \qquad \mathbf{S}_n = (\mathbf{A} - \mathbf{I})\mathbf{S}_a(\mathbf{A} - \mathbf{I})^{\mathbf{T}}$$

and

$$\mathbf{G} = \left(\mathbf{K}^{\mathbf{T}}\mathbf{S}_y^{-1}\mathbf{K} + \mathbf{S}_a^{-1}\right)^{-1}\mathbf{K}^{\mathbf{T}}\mathbf{S}_y^{-1}, \qquad \mathbf{A} = \mathbf{GK}.$$

[29] We can use the error ratio σ/σ_a, where σ^2 and σ_a^2 are the diagonal components of $\mathbf{S}$ and $\mathbf{S}_a$, respectively. We may say that $\mathbf{S}_m$ is a measurement error and $\mathbf{S}_n$ is a smoothing error, as will be shown in Figure 10. We estimate the precision retrieved from single-scan data for O_3, HCl, HNO_3, HOCl, BrO, ClO, and HO_2 based on our algorithm and sensor specifications (Figure 5). O_3, HCl, HNO_3, and HOCl are estimated from Band A, and ClO, BrO, and HO_2 are estimated from Band C. A priori profiles of those molecules are assumed to be the annual averaged daytime profiles of Aura/MLS ver. 2.2 data in the midlatitudes (40°N) for O_3, HCl, HNO_3, ClO, and HO_2, and the Center for Climate System Research (CCSR)/National Institute for Environmental Studies (NIES) data based on the model output of the CCSR/NIES Chemistry Coupling Model [*Akiyoshi et al.*, 2009] for BrO and HOCl at noon. We also use the data for profiles of temperature, humidity, and wind from the Goddard Earth Observing System-5 (GEOS-5) assimilated data products provided by the Global Modeling and Assimilation Office at NASA's Goddard Space Flight Center [*Rienecker et al.*, 2007]. The standard deviations of a priori profiles are assumed to be 100% of their mean values for all species. The definition of the noise level of spectra is the same as that in section 3.3 [equation (1)]. Here we assume that the system noise is 350 K, τ is 0.5 s, and $\Delta\nu$ is 2.5 MHz. The other parameters such as the antenna pattern, AOS response function, and transmission function of the sideband separator are based on the measured values.

[30] Profiles of O_3, HCl, and ClO can be retrieved with RMS errors of less than 10% between 20 and 60 km (O_3 and HCl) and 25 and 45 km (ClO). Knowledge of spectroscopic parameters will limit the product accuracy for O_3, HCl, and ClO. Other species can be retrieved with 20%–50% precision. Retrieval of weaker lines, such as BrO, can only have error ratios as high as 50%. We carefully examine the effect of a priori values on the retrieval results if the error ratio >0.5. An averaging algorithm avoiding a priori bias [*Livesey et al.*, 2006b] will be applied for the weak species, such as BrO and HO_2.

5. Acquired Data and First Results

[31] The following results are mostly based on Version 0032 of the SMILES operational product, which was released to internal researchers as the second release version in April 2010; the first one (Version 0024) was released in January 2010. The Version 0032 product is basically similar to Version 0024, but we tried to retrieve all the available profiles. Although some inappropriate data are included, we can get a larger number of usable profiles than we could from Version 0024. Data access is allowed under the condition of submitting a research proposal. (More information is available at http://smiles.tksc.jaxa.jp/indexe.shtml.)
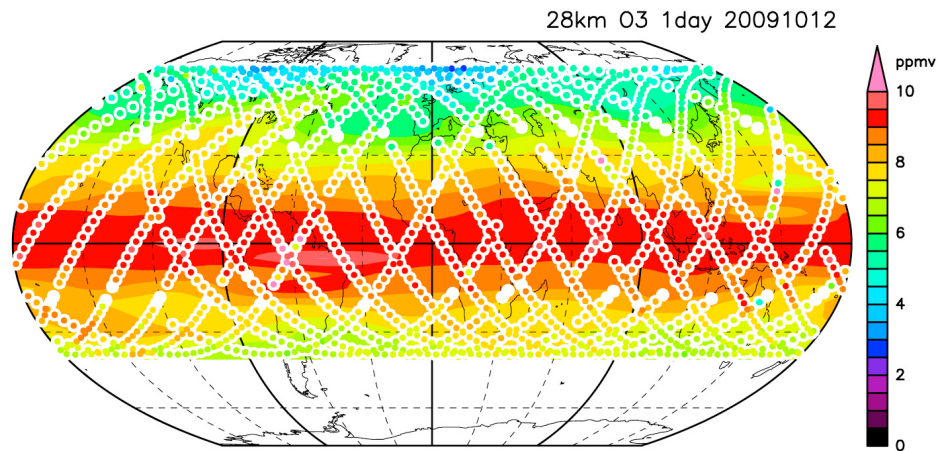
Figure 6. Globally mapped ozone distributions at 28 km on 12 October 2009. Original observation points are plotted by white circles with observed ozone mixing ratios.

[32] Ozone retrieval is performed using Band A and Band B. As the ozone lines in the two bands are strong, it is rather easy to get reasonable results. However, uncertainty may still exist in the spectral parameters, and we need further improvement of the retrieval algorithm for precise outputs. Figure 6 shows horizontal ozone distributions at 28 km on 12 October 2009, the first day of the SMILES global observation. On the gridded map as a background, observation points with white circles are overlain. The gridded data of SMILES were constructed by Fourier forward and backward transformation of the data for a single day with maximum wave numbers of 6 along latitudinal circles with 5° intervals. There are higher ozone mixing ratios in low latitudes, and they decrease as the latitude increases. As mentioned in subsection 3.2, SMILES observations sometimes suffer from interference due to the solar paddle, and we see some missing data along specific latitude bands, in this case around 15°S and 35°N, in each ascending and descending mode.

[33] By averaging along the latitudinal band with 5° intervals, the latitude-height section of the zonal mean ozone derived from SMILES is drawn in Figure 7 (left). This can be readily compared with that from MLS on the same day (Figure 7, right). See *Froidevaux et al.* [2008] for MLS ozone data quality. The subtropical maxima around 15°N and 15°S at about 30 km are identical in these two plots.
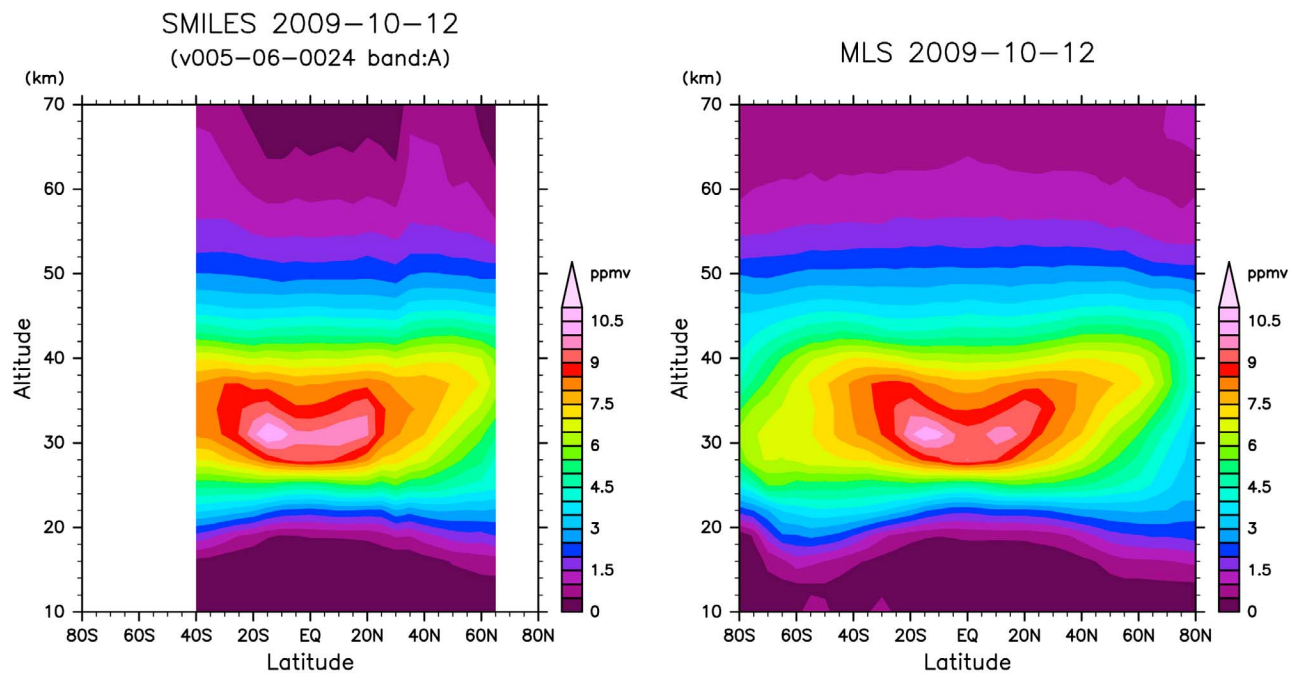

Figure 7. Latitude-height sections of the zonal mean ozone on 12 October 2009 from (left) SMILES and (right) MLS. Data for daytime and nighttime are averaged.
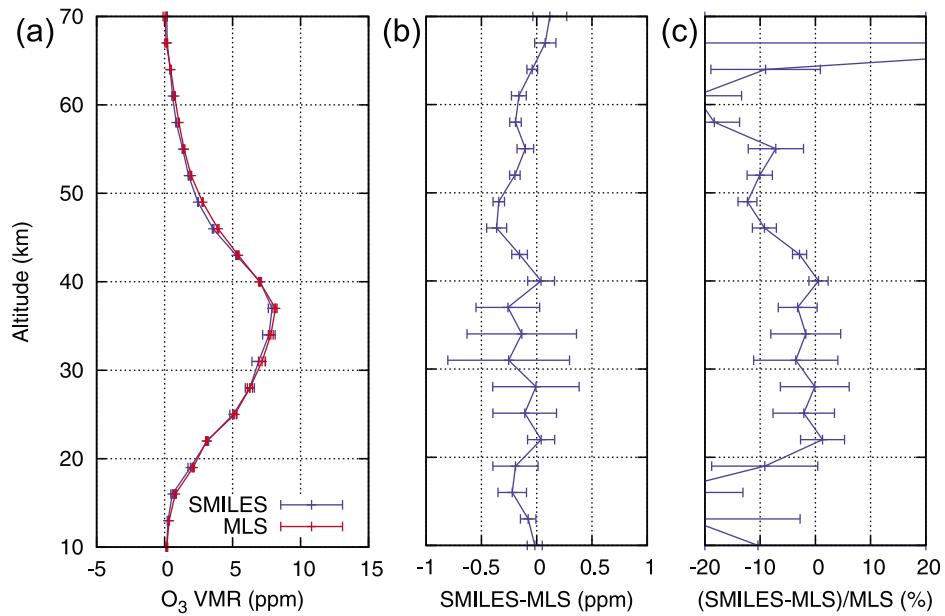
Figure 8. Comparison of coincident SMILES and MLS ozone profiles on 12 October 2009 at northern high latitudes: (a) the mean profiles for SMILES (blue) and MLS (red), (b) the differences between the SMILES and MLS profiles in mixing ratio, and (c) the percentage differences.

However, around 30°N in particular, some strange discontinuities can be seen owing to the solar paddle interference, as indicated in Figure 6, suggesting that we need further careful treatment to confirm data quality.

[34] As to the two maxima of ozone mixing ratios, it is suggested that the distribution is affected by the meridional circulation associated with the quasi-biennial oscillation (QBO) in the equatorial stratosphere. Analysis fields indicate that vertical wind shear is westerly around this height and time, and it is expected that vertical motion with sinking at the equator should dominate [*Plumb and Bell*, 1982]. Such a downward displacement of material surface was clearly
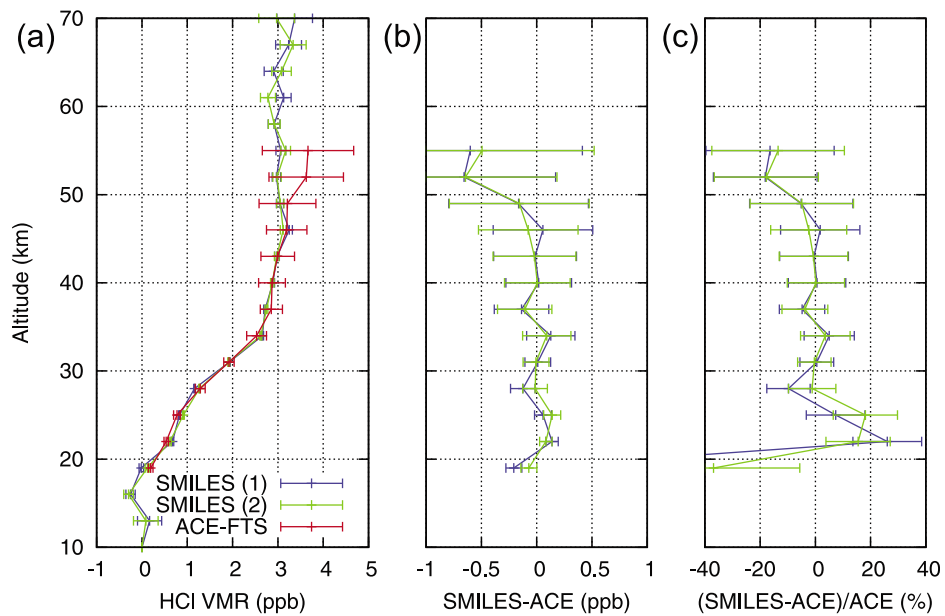

Figure 9. An example of HCl profiles from SMILES and a comparison with that from ACE-FTS: (a) two profiles from SMILES on 12 October 2009, (1) at 5.1°N and 166.5°E (blue), (2) at 7.7°N and 168.4°E (green), and one profile from ACE on 13 October 2009 at 5.2°N and 170.7°E (red) within 24 hr and a distance of 500 km, (b) the differences between the SMILES and ACE profiles in mixing ratio, and (c) the percentage differences.
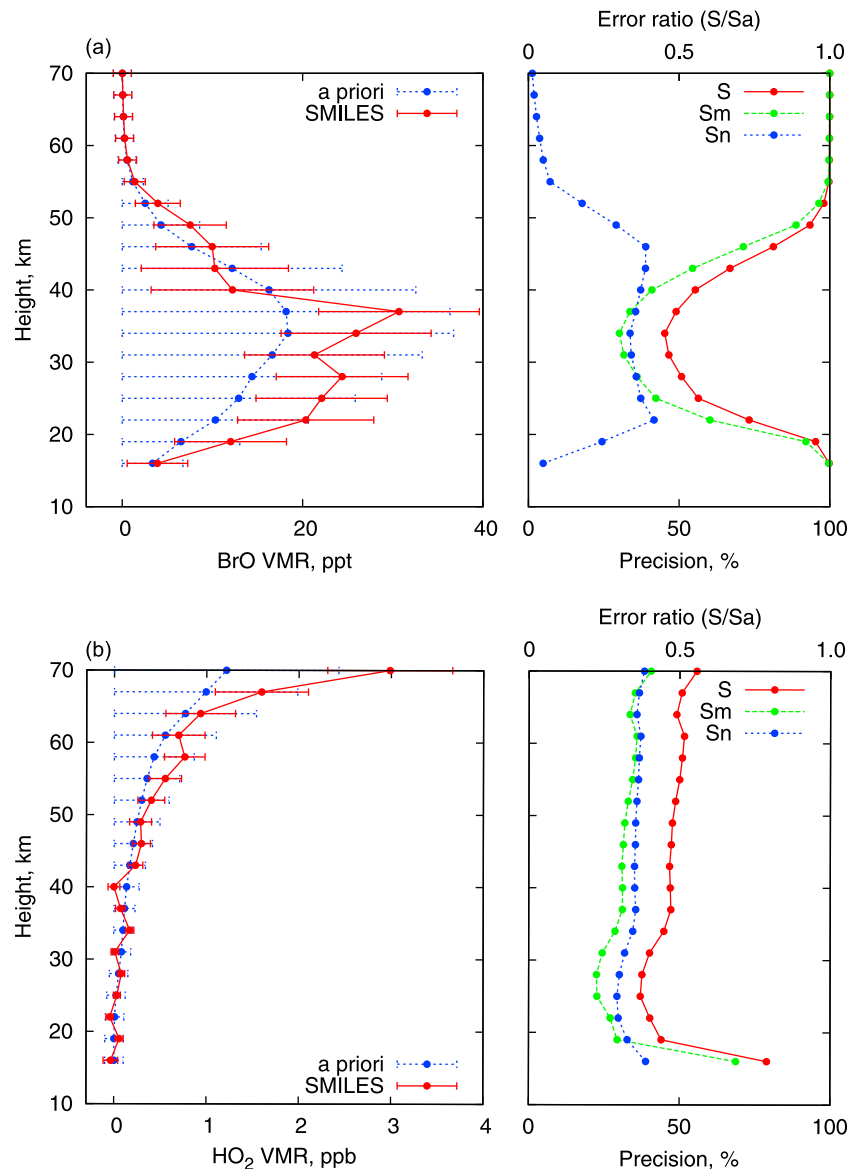
Figure 10. Examples of the retrieved and a priori profiles for (a) BrO and (b) HO$_2$. Left: Marks and horizontal bars indicate retrieved values and one standard deviation in red, and those for the a priori profile in blue. Right: S, total error; Sm, measurement error; Sn, smoothing error.

seen in satellite aerosol data [*Trepte and Hitchman*, 1992]. Because of this downward displacement, in conjunction with warm anomalies, ozone variations related to the QBO around 30 km show minima at the equator when the QBO is in the westerly shear [e.g., *Shiotani and Hasebe*, 1994]. Thus, the latitude-height cross section shows a dip over the equator above the ozone maxima and two peaks of ozone concentrations at subtropical latitudes, as shown by *Randel and Wu* [1996] using the monthly mean satellite data.

[35] Comparisons of coincident SMILES and MLS ozone profiles are shown in Figure 8. In northern high latitudes on 12 October 2009, there are four SMILES profiles for which we can find corresponding MLS profiles within 500 km and 1 hr. The SMILES profiles are mostly located at high latitudes, 47.9°N and 127.2°W, 48.2°N and 81.1°W, 50.6°N and 84.5°W, and 57.1°N and 142.8°W, and the numbers of

the MLS coincidences are 5, 6, 6, and 1, respectively. In Figure 8a, the mean ozone profiles are drawn in blue for SMILES (four observations) and red for MLS (18 observations); the ozone peak is elevated in comparison with that at low latitudes. The difference between the two in mixing ratio (SMILES–MLS) and the percentage difference [(SMILES–MLS)/MLS] are calculated and shown in Figures 8b and 8c, respectively. The overall agreement is good, within 5% for the height range of about 20–45 km.

[36] The retrieval for HCl is based on Band A and Band B. Figure 9 shows an example of HCl profiles from Band A and their comparison with Atmospheric Chemistry Experiment (ACE) Fourier transform spectrometer (FTS) data [*Mahieu et al.*, 2008] under rather loose criteria within a distance of 500 km and a time of 24 hr. We found two to three coincidences per day with ACE-FTS, and this figure

shows a coincidence case in the first day for SMILES. It is found that the SMILES profiles and the ACE-FTS profile agree very well within 10% for the height range of 25–50 km. It should be noted that the two SMILES profiles fit within the error bars of the ACE-FTS in the altitude region for 25–50 km. We have been conducting extensive comparisons for validation, and the results will be summarized in separate papers.

[37] Finally, we will briefly show profiles for BrO and HO_2, which were thought to be rather difficult species to retrieve using a single scan; however, we found that the result is reasonable, though the error ratio is larger than that for species with strong spectral peaks. Figure 10 shows examples of the retrieved profiles for BrO and HO_2 from the single scan. The two profiles remain separate from the a priori profile and contain enough information to be retrieved. We found that the daily zonal mean is enough to capture the height distribution of these species, since the local time changes only about 22 minutes a day owing to ISS orbit characteristics. By combining the ascending and descending measurements, diurnal variations of these minor constituents can be seen in about a month. Thus, SMILES can measure the atmosphere at different local times, and observational results for the diurnal variation of these minor constituents will provide further insight into atmospheric chemistry. Such observational results will be described in separate papers as well.

6. Summary

[38] The Superconducting Submillimeter-Wave Limb-Emission Sounder (SMILES) was successfully launched on 11 September 2009, started atmospheric observations on 12 October and has been performing global observations at about 100 points per ISS orbit, except for some restrictions due to ISS operation. This is an outstanding experiment that is retrieving unique data with lower noise than other instruments because it employs a 4 K mechanical cooler and superconducting mixers for limb-emission soundings in the submillimeter-wave range. The spectra are used to retrieve vertical profiles of the atmospheric minor constituents in the middle atmosphere (O_3, HCl, ClO, HO_2, HOCl, BrO, O_3 isotopes, HNO_3, CH_3CN, etc.) with their diurnal variations, which will contribute to various issues of atmospheric science.

[39] We have presented some preliminary results. The derived profiles and horizontal distributions of ozone and HCl are reasonable, though we need further improvement of the retrieval algorithm for precise outputs. Even for those species with weak signals, such as BrO and HO_2, we can get promising results, even for a single scan. Averaging, such as daily zonal means, will produce scientifically useful signal-to-noise ratios for these species. We have shown the capability of obtaining high-quality scientific data that will be important to addressing scientific issues such as the ozone trend problem, middle atmosphere chemistry with a special focus on the diurnal cycle, and the transport process of minor species. These outcomes from SMILES will demonstrate its high potential to observe atmospheric minor constituents in the middle atmosphere.

[40] There are several studies in progress that will develop the analysis further from the viewpoint of extensive comparisons for the validation and new scientific achievements, particularly on the diurnal variation of some minor species.

References

Akiyoshi, H., L. B. Zhou, Y. Yamashita, K. Sakamoto, M. Yoshiki, T. Nagashima, M. Takahashi, J. Kurokawa, M. Takigawa, and T. Imamura (2009), A CCM simulation of the breakup of the Antarctic polar vortex in the years 1980–2004 under the CCMVal scenarios, *J. Geophys. Res.*, *114*, D03103, doi:10.1029/2007JD009261.

Buehler, S. A. (1999), Microwave limb sounding of the stratosphere and upper troposphere, Ph.D. thesis, 262 pp., Univ. of Bremen, Bremen, Germany.

Buehler, S. A., A. von Engeln, P. Eriksson, T. Kuhn, C. Verdes, and K. Kunzi (1999), Superconducting Sub-millimeter Wave Limb-Emission Sounder SMILES, *Proc. IEEE 1999 Int. Geosci. Remote Sens. Symp.*, *1*, 497–499.

Buehler, S. A., C. L. Verdes, S. Tsujimaru, A. Kleinböhl, H. Bremer, M. Sinnhuber, and P. Eriksson (2005), Expected performance of the Superconducting Submillimeter-Wave Limb-Emission Sounder compared with aircraft data, *Radio Sci.*, *40*, RS3016, doi:10.1029/2004RS003089.

Canty, T., H. M. Pickett, R. J. Salawitch, K. W. Jucks, W. A. Traub, and J. W. Waters (2006), Stratospheric and mesospheric HO_x: Results from Aura MLS and FIRS-2, *Geophys. Res. Lett.*, *33*, L12802, doi:10.1029/2006GL025964.

De Laeter, J. R., J. K. Böhlke, P. De Bièvre, H. Hidaka, H. S. Peiser, K. J. R. Rosman, and P. D. P. Taylor (2003), Atomic weights of the elements: Review 2000 (IUPAC Technical Report), *Pure Appl. Chem.*, *75*(6), 683–800, doi:10.1351/pac200375060683.

Eyring, V., et al. (2007), Multimodel projections of stratospheric ozone in the 21st century, *J. Geophys. Res.*, *112*, D16303, doi:10.1029/2006JD008332.

Frisk, U., et al. (2003), The Odin satellite. I. Radiometer design and test, *Astron. Astrophys.*, *402*, L27–L34, doi:10.1051/0004-6361:20030335.

Froidevaux, L., et al. (2008), Validation of Aura Microwave Limb Sounder stratospheric ozone measurements, *J. Geophys. Res.*, *113*, D15S20, doi:10.1029/2007JD008771.

Hartmann, G. K., et al. (1996), Measurements of O_3, H_2O, and ClO in the middle atmosphere using the millimeter-wave atmospheric sounder (MAS), *Geophys. Res. Lett.*, *23*(17), 2313–2316.

Imai, K., M. Suzuki, and C. Takahashi (2010), Evaluation of Voigt algorithms for the ISS/JEM/SMILES L2 data processing system, *Adv. Space Res.*, *45*, 669–675.

Inatani, J., S. Ochiai, T. Manabe, M. Seta, R. Wylde, and D. H. Martin (1999), A new configuration of the Martin-Puplett interferometer with low reflection, paper presented at IEEE Seventh International Conference on Terahertz Electronics Proceedings, Nara, Japan, 1999.

Inatani, J., et al. (2000), Submillimeter Limb-emission Sounder JEM/SMILES aboard the Space Station, *Proc. SPIE*, *4152*, 243–254.

Jarnot, R. F., V. S. Perun, and M. J. Schwartz (2006), Radiometric and spectral performance and calibration of the GHz bands of EOS MLS, *IEEE Trans. Geosci. Remote Sens.*, *44*(5), 1131–1143.

Kasai, Y., C. Takahashi, S. Tsujimaru, S. Ochiai, S. Buehler, K. Takahashi, T. Shirai, H. Ozeki, and H. Masuko (2000), JEM/SMILES limb-sounding of stratospheric trace species II: Simulation results for JEM/SMILES observations, *Proc. SPIE*, *4152*, 263–273.

Kasai, Y., J. Urban, C. Takahashi, S. Hoshino, K. Takahashi, J. Inatani, M. Shiotani, and H. Masuko (2006), Stratospheric ozone isotope enrichment studied by submillimeter wave heterodyne radiometry: The observation capabilities of SMILES, *IEEE Trans. Geosc. Remote Sens.*, *44*(3), 676–693.

Koga, K., T. Goka, H. Matsumoto, Y. Muraki, K. Masuda, and Y. Matsubara (2001), Development of the fiber neutron monitor for the energy range 15–100 MeV on the International Space Station (ISS), *Radiat. Meas.*, *33*, 287–291.

Kovalenko, L. J., et al. (2007), Observed and modeled HOCl profiles in the midlatitude stratosphere: Implication for ozone loss, *Geophys. Res. Lett.*, *34*, L19801, doi:10.1029/2007GL031100.

Krankowsky, D., P. Lämmerzahl, K. Mauersberger, C. Janssen, B. Tuzson, and T. Röckmann (2007), Stratospheric ozone isotope fractionations derived from collected samples, *J. Geophys. Res.*, *112*, D08301, doi:10.1029/2006JD007855.

Levenberg, K. (1944), A method for the solution of certain problems in least squares, *Q. Appl. Math*, *2*, 164–168.

Livesey, N. J., L. J. Kovalenko, R. J. Salawitch, I. A. MacKenzie, M. P. Chipperfield, W. G. Read, R. F. Jarnot, and J. W. Waters (2006a), EOS Microwave Limb Sounder observations of upper stratospheric BrO: Implications for total bromine, *Geophys. Res. Lett.*, *33*, L20817, doi:10.1029/2006GL026930.

Livesey, N. J., W. V. Snyder, W. G. Read, and P. A. Wagner (2006b), Retrieval algorithms for the EOS Microwave Limb Sounder (MLS) instrument, *IEEE Trans. Geosci. Remote Sens.*, *44*(5), 1144–1155.

Mahieu, E., et al. (2008), Validation of ACE-FTS v2.2 measurements of HCl, HF, CCl$_3$F, and CCl$_2$F$_2$ using space-, balloon- and ground-based instrument observations, *Atmos. Chem. Phys.*, *8*, 6199–6221.

Manabe, T., J. Inatani, A. Murk, R. J. Wylde, M. Seta, and D. H. Martin (2003), A new configuration of polarization-rotating dual-beam interferometer for space use, *IEEE Trans. Microwave Theory Tech.*, *51*(6), 1696–1704.

Manabe, T., T. Fukami, T. Nishibori, K. Mizukoshi, and S. Ochiai (2008), Measurement and evaluation of submillimeter-wave antenna quasioptical feed system by a phase-retrieval method in the 640 GHz band, *IEICE Trans. Comm.*, *E91-B*(6), 1760–1766.

Manabe, T., T. Nishibori, K. Mizukoshi, F. Ohtsubo, and S. Ochiai (2010), Measurements of the offset Cassegrain antenna of JEM/SMILES using a near-field phase-retrieval method in the 640 GHz band, paper presented at 21st International Symposium Space Terahertz Technology, Oxford, U.K., March 23–25, 2010.

Marquardt, D. W. (1963), An algorithm for the least-squares estimation of nonlinear parameter, *J. Soc. Ind. Appl. Math.*, *11*(2), 431–441.

Masuko, H., S. Ochiai, Y. Irimajiri, J. Inatani, Y. Noguchi, Y. Iida, N. Ikeda, and N. Tanioka (1997), A Superconducting Submillimeter-Wave Limb-Emission Sounder (SMILES) on the Japanese Experimental Module (JEM) of the Space Station for observing trace gases in the middle atmosphere, paper presented at Eighth International Symposium on Space Terahertz Technology, Harvard Univ., Cambridge, Mass., March 25–27, 1997.

Masuko, H., et al. (2000), Superconducting Submillimeter-Wave Limb-Emission Sounder (SMILES) onboard Japanese Experimental Module (JEM) of International Space Station (ISS), in *Proc. IEEE 2000 Int. Geosci. Remote Sens. Symp.*, *1*, 71–73.

Melsheimer, C., et al. (2005), Intercomparison of general purpose clear sky atmospheric radiative transfer models for the millimeter/submillimeter spectral range, *Radio Sci.*, *40*, RS1007, doi:10.1029/2004RS003110.

Mihara, T., et al. (2000), MAXI (Monitor of All-sky X-ray Image) for JEM on the International Space Station, *Adv. Space Res.*, *25*(3/4), 897–900.

Murtagh, D. U., et al. (2002), An overview of the Odin atmospheric mission, *Can. J. Phys.*, *80*, 309–319.

Narasaki, K., S. Tsunematsu, S. Yajima, A. Okabayashi, J. Inatani, K. Kikuchi, R. Satoh, T. Manabe, and M. Seta (2004), Development of cryogenic system for SMILES, *AIP Conf. Proc.* *710*(1), 1785–1796.

Ochiai, S., S. Tsujimaru, Y. Irimajiri, T. Manabe, and I. Murata (2005), Stratospheric ozone and ClO measurement using balloon-borne submillimeter limb sounder, *IEEE Trans. Geosci. Remote Sens.*, *43*(6), 1258–1265.

Onaka, T., and T. Nakagawa (2005), SPICA: A 3.5 m space infrared telescope for mid- and far-infrared astronomy, *Adv. Space Res.*, *36*, 1123–1127.

Ozeki, H., Y. Kasai, S. Ochiai, S. Tsujimaru, J. Inatani, H. Masuko, C. Takahashi, L. Mazuray, and C. Rosolen (2000), Submillimeter wave spectroscopy performance of JEM/SMILES, *Proc. SPIE*, *4152*, 255–262.

Plumb, R. A., and R. C. Bell (1982), A model of the quasi-biennial oscillation on an equatorial beta-plane, *Q. J. R. Meteorol. Soc.*, *108*, 335–352.

Randel, W. J., and F. Wu (1996), Isolation of the ozone QBO in SAGE II data by singular value decomposition, *J. Atmos. Sci.*, *53*, 2546–2559.

Rienecker, M. M., et al. (2007), The GEOS-5 data assimilation system: Documentation of versions 5.0.1, 5.1.0, and 5.2.0, *Tech. Rep. Ser. on Global Modeling and Data Assimilation*, NASA/TM-2007-104 606, 27.

Rodgers, C. D. (1976), Retrieval of atmospheric temperature and composition from remote measurements of thermal radiation, *Rev. Geophys.*, *14*(4), 609–624.

Rodgers, C. D. (1990), Characterization and error analysis of profiles retrieved from remote sounding measurements, *J. Geophys. Res.*, *95*(D5), 5587–5595.

Rodgers, C. D. (2000), *Inverse Methods for Atmospheric Sounding: Theory and Practice, Ser. on Atmos., Oceanic, and Planet. Phys.*, vol. 2, World Scientific, Singapore.

Salawitch, R. J., D. K. Weisenstein, L. J. Kovalenko, C. E. Sioris, P. O. Wennberg, K. Chance, M. K. W. Ko, and C. A. McLinden (2005), Sensitivity of ozone to bromine in the lower stratosphere, *Geophys. Res. Lett.*, *32*, L05811, doi:10.1029/2004GL021504.

Seta, M., et al. (2000), Submillimeter-wave SIS receiver for JEM/SMILES, *Adv. Space Res.*, *26*(6), 1021–1024.

Shiotani, M., and F. Hasebe (1994) Stratospheric ozone variations in the equatorial region as seen in Stratospheric Aerosol and Gas Experiment data, *J. Geophys. Res.*, *99*(D7), 14,575–14,584.

Sinnhuber, B.-M., et al. (2005), Global observations of stratospheric bromine monoxide from SCIAMACHY, *Geophys. Res. Lett.*, *32*, L20810, doi:10.1029/2005GL023839.

Takahashi, C., et al. (2000), JEM/SMILES limb-sounding of stratospheric trace species I: Retrieval algorithm and simulator, *Proc. SPIE*, *4152*, 274–282.

Takahashi, C., S. Ochiai, and M. Suzuki (2010), Operational retrieval algorithms for JEM/SMILES level 2 data processing system, *J. Quant. Spectrosc. Radiat. Transfer*, *111*, 160–173.

Takahashi, T., et al. (2008), The Next mission, *Proc. SPIE*, *7011*, 70110O.

Trepte, C. R., and M. H. Hitchman (1992), Tropical stratospheric circulation deduced from satellite aerosol data, *Nature*, *355*, 626–628.

Verdes, C. (2002), Deriving atmospheric temperature and instrumental pointing from millimeter/sub-millimeter limb sounding measurements, Ph.D. thesis, 131 pp., Univ. of Bremen, Bremen, Germany.

Waters, J. W., et al. (2006), The Earth Observing System Microwave Limb Sounder (EOS MLS) on the Aura Satellite, *IEEE Trans. Geosci. Remote Sens.*, *44*(5), 1175–1092.

World Meteorological Organization (WMO) (1999), *Scientific Assessment of Ozone Depletion: 1998, Global Ozone Research and Monitoring Project, Rep. 44*, Geneva, Switzerland.

World Meteorological Organization (WMO) (2007), *Scientific Assessment of Ozone Depletion: 2006, Global Ozone Research and Monitoring Project, Rep. 50*, Geneva, Switzerland.

J. Inatani, National Astronomical Observatory of Japan, Mitaka, Japan.

Y. Irimajiri, Y. Kasai, H. Masuko, Y. Murayama, and S. Ochiai, National Institute of Information and Communications Technology, Koganei, Japan.

K. Kikuchi, K. Mizukoshi, T. Nishibori, R. Sato, and M. Takayanagi, ISS Science Project Office, Tsukuba Space Center, Japan Aerospace Exploration Agency, Tsukuba, Japan.

M. Koike, Department of Earth and Planetary Physics, Graduate School of Science, University of Tokyo, Tokyo, Japan.

T. Manabe, Department of Aerospace Engineering, Graduate School of Engineering, Osaka Prefecture University, Sakai, Japan.

T. Nagahama, Solar-Terrestrial Environment Laboratory, Nagoya University, Nagoya, Japan.

H. Ozeki, Department of Environmental Science, Faculty of Science, Toho University, Funabashi, Japan.

T. Sano, M. Suzuki, and C. Takahashi, ISS Science Project Office, Institute of Space and Astronautical Science, Japan Aerospace Exploration Agency, Sagamihara, Japan.

M. Seta, Institute of Physics, University of Tsukuba, Tsukuba, Japan.

M. Shiotani, Research Institute for Sustainable Humanosphere, Kyoto University, Gokasho, Uji, Kyoto 611-0011, Japan. (shiotani@rish.kyoto-u.ac.jp)